regulation; the cytotoxic drugs can be delivered separately or con-currently with the inhibitors to the tumor sites via the administration of the nanoparticles. In line with these approaches, several studies have recently been reported with the goal of overcoming MDR through the specific inhibition of MDR proteins. Nanoparticles containing a combination of cytotoxic drugs and efflux pump inhibitors, such as cyclosporine, verapamil, and tariquidar, have shown promise in terms of reversing MDR in cancer cells (Patil et al. 2009; Soma et al. 2000; Wu et al. 2007). Nanoparticles co-encapsulated with cyclosporin A and DOX result in about two folds higher efficacy in DOX-resistant leukemia cells as compared to free cyclosporin A or only DOX-loaded particles (Soma et al. 2000). In another study, it was depicted that transferrin-conjugated liposomes containing both verapamil and DOX were expedited cellular internalization, resulting in a higher accumulation of DOX in a DOX-resistant leukemia cell line (K562), and thereby demonstrated the reversal of MDR as compared to the use of unmodified liposomes (Wu et al. 2007). In addition, biotin-conjugated poly lactic-co-glycolic acid (PLGA) nanoparticles loaded with paclitaxel and tariquidar, also showed improved therapeutic efficacy in breast cancer, as compared to the non-targeted formulations (Patil et al. 2009). Despite the immense role of MRP and BCRP on mediating MDR in cancer cells, the application of nanoparticles loaded with inhibitors aimed at suppressing the function of these proteins have not been extensively studied. As a potent GST inhibitor, ethacrynic acid was reported to efficiently potentiate the cytotoxic effects of chlorambucil and melphalan in human colon cancer cell lines (Clapper et al. 1990). Thus the use of nanoparticles loaded with this inhibitor and a cytotoxic drug would be a promising tool for overcoming the resistance of cancer cells where GST plays a pivotal role. Based on the above information, it is evident that the targeted delivery of chemosensitizers (inhibitors) and chemotherapeutics via the utilization of nanoparticles promises to be a safer and effective approach to the treatment of cancers that are resistant to chemotherapy.

Delivery of nucleic acids aimed to target MDR proteins

Gene delivery, aimed to controlling the activity of a specific gene via RNA interference (RNAi), has become a powerful tool in cancer therapeutics. RNAi is a post-transcriptional gene silencing mechanism that is mediated by small interfering RNAs (siRNAs) of 21–25 nucleotides (nt) (Filipowicz et al. 2005). The double-stranded RNA molecules are incorporated into the RNA-induced silencing complex (RISC), where they induce the degradation of target mRNAs in a sequence-specific manner (Filipowicz et al. 2005). In solid tumors, membrane transporter families play a pivotal role in the distribution and excretion of clinically applicable chemotherapeutic drugs (Fig. 1). In recent years, several attempts to control the expression of ABC transporters by delivering nucleic acids (siRNA, miRNA etc.) loaded with nanoparticles to tumors have been made (Patil and Panyam 2009; Wang et al. 2010), as illustrated in Fig. 2B. In MDR cancer therapy, siRNA has been used to down-regulate MDR-related proteins by silencing MDR-1 (Liu et al. 2009), MRP1 and Bcl-2 (Saad et al. 2008). Nanoparticles loaded with P-gp siRNA and DOX were applied to the delivery of encapsulated contents into tumors (Meng et al. 2010) where the delivered siRNA silences the expression of P-gp which consequently increases the intracellular concentration of DOX. Following the same purpose, specific ligand modified liposomes containing P-gp siRNA or DOX were also used to treat drug resistant tumors (Jiang et al. 2010). Nanoparticles loaded with MDR-siRNAs showed enhanced gene transfection (Nakamura et al. 2011), which can be attributed to its systemic stability as well as target specificity, as compared to free siRNAs which are unstable in serum and show poor cellular uptake (Gao et al. 2009). In addition, ligand modified nanoparticles also capable to addressing the off targeting issue in siRNA delivery (Di Paolo et al. 2011), which is a prerequisite for down regulating the specific genes present in the MDR tumor tissues.

It was also reported that the co-delivery of paclitaxel and Bcl-2-targeted siRNA from cationic amphiphilic copolymeric self-assembled nanoparticles exhibited superior activity in a breast cancer cell line (MDA-MB-231) via the down regulation of Bcl-2 expression, as compared to the individual agents (Wang et al. 2006). In another study, it was reported that paclitaxel and P-gp siRNA loaded in PLGA-polyethyleneimine (PEI) copolymeric nanoparticles resulted in significantly higher paclitaxel retention in MDR cancer cells and a better activity in vivo (Patil et al. 2010), which showed minimal response to paclitaxel without silencing the P-gp. Liposomes loaded with DOX as well as MRP-1 and Bcl-2 siRNAs caused the induction of cell apoptosis as well as the reversal of MDR in lung cancer (H69AR, human SCLC) (Saad et al. 2008). Recently, a dual-sequential treatment strategy was applied in which siRNA and drug loaded bispecific antibodies (BsAb) modified targeted micelles were delivered to knockdown the expression of MDR1 (MacDiarmid et al. 2009), where the tumors were treated with siRNA loaded minicells followed by the administration of minicells loaded with shRNA. The subsequent administration of drug (5-FU and irinotecan) loaded targeted minicells showed a better pharmacological effect against drug resistant tumors. Furthermore, simultaneous administration of anti-MDR1 shRNA encoding vectors as well as DOX inhibited tumor growth by reversing MDR (Walther et al. 2010). Survivin

is a negative regulator of apoptosis and its expression is elevated in MDR cancer cells (Fig. 1). Therefore, inhibiting the expression of survivin would likely be effective in enhancing apoptosis in cancer cells (Kanwar et al. 2011). Considering this issue, polyamidoamine (PAMAM) dendrimer modified magnetic nanoparticles were used to deliver antisense oligodeoxynucleotides (asODN) with the objective of suppressing the survivin mRNA and protein levels in breast cancers (MCF-7 and MDA-MB-435) and in liver cancer (HepG2) cells. The above preparations showed the resensitization of MDR cancer cells to the drug molecules where they were initially resistant. Therefore, prier to delivering the cytotoxic drug to MDR cancer cells, it is immensely important to control the level of expressions of the respective genes (Fig. 2B) by delivering the nucleic acids via the nanoparticles.

Delivery of nanoparticles to modulate the uptake route of drugs

Drugs that are encapsulated in nanoparticles have different pharmacokinetic properties compared to the free drugs. Free drugs are generally internalized by diffusion across the cellular membrane and the drug efflux pumps present on the cell membrane can sense free drug molecules as they cross the membrane (Fig. 2C), and prevent them from entering the cell cytoplasm or making them vulnerable to capture by ABC transporters, with their subsequent ejection. To overcome the problems associated with the efflux of free drugs as well as to increase their efficacy, nanocarriers would be the effective tool where the drugs can be loaded or encapsulated and can deliver the payload to the cellular internal organelles (Fig. 2C). Nanocarriers are internalized into cells via a non-specific endocytosis pathway and cross the cell membrane in an 'invisible' form, thereby preventing the drugs from being recognized by efflux pumps (Huwyler et al. 2002, Rejman et al. 2004). This type of endocytosis process is called "stealth endocytosis" (Fig. 2C), and results in a higher intracellular accumulation of the drug (Davis et al. 2008). The particles are internalized in endosomes that release drugs near the peri-nuclear region (or deep inside the cytoplasm) away from membrane ABC transporters (Shen et al. 2008). Following these steps, nanocarriers are able to bypass ABC transporters (Fig. 2) (Kunjachan et al. 2012) and the cytotoxic drugs are shielded from cytoplasmic detoxification enzymes such as MT and methionine synthase (Murakami et al. 2011). It was reported that taxol-containing liposomes exhibited antitumor effects in a taxol-resistant Colon-26 tumor model (Sharma et al. 1993). In addition, polymer-drug conjugate comprised of a paclitaxel-carboxymethyl dextran exhibited the in vivo antitumor activity against paclitaxel-resistant Colon-26 carcinoma cells (Sugahara et al. 2007). Therefore, by modulating the uptake route as well as by targeting subcellular compartments, DDSs utilizing nanocarriers would be the effective tool for reversing MDR in cancer cells.

Targeted anti-angiogenic therapy

For the growth and progression of a tumor, the tumor cells need glucose, minerals, and oxygen which are initially supplied by nearby blood vessels; but as the tumor grows, the cells in the interior of the tumor become farther away from the blood supply. To continue growing, tumor must have new blood vessels. Without the formation of new blood vessels, a tumor can not grow larger than about 1–2 mm^3 (Bamias and Dimopoulos 2003). With the help of several key promoters secreted from the tumor cells, the new blood vessels are formed within the tumor microenvironment from pre-existing blood vessels, a process called tumor angiogenesis (Folkman 1995). To control the growth of tumors, several attempts have been made to inhibit tumor angiogenesis, a process that involves down-regulating key promoters as well as by delivering cytotoxic drugs to the tumor endothelial cells (TECs) present in the tumor blood vessels (Fig. 2D), a process that is referred to as anti-angiogenic therapy (Folkman 2007; Jain 2005). Tumor vasculatures are generally leaky, with endothelial cell gaps of ~100–600 nm (Hashizume et al. 2000), although the length of cell gaps depend on the tumor type, malignancy, and the stage of the disease (Hashizume et al. 2000; Hobbs et al. 1998; Siwak et al. 2002). Nanoparticles with diameters of ~100 nm (dnm) are used to target the tumor tissues which accumulate in tumor cells through the leaky tumor vasculature via the enhanced permeability and retention (EPR) effect (Maeda et al. 2000), a universal phenomenon in solid tumors (with some exceptions in the case of hypovascular tumors, such as prostate cancer or pancreatic cancer). Nanoparticles with dnm smaller than 10 cross the basement membranes in the glomeruli of kidneys and are rapidly cleared, which leads to a shorter blood half-life (Choi et al. 2010). Therefore, a particle size of 10–100 dnm would be suitable for in vivo tumor targeting based on the EPR effect (Gupta and Gupta 2005). Doxil, a typical successful example of a DOX loaded small size PEG-LP (~100 dnm), functions against tumor cells via the EPR effect, and is used clinically in the treatment of breast cancer, ovarian cancer, AIDS related Kaposi's sarcoma etc. (Haley and Frenkel 2008; Yuan et al. 1994). However, it shows very poor or even no therapeutic efficacy against the cancers that are resistant to DOX. This circumstance is also true for other types of chemotherapeutic drugs once the cancer cells become resistant to them. Tumors that are resistant to chemotherapy would be difficult to treat by delivering drugs to the tumor cells. Therefore, an alternate approach for treating drug-resistant cancers would be highly

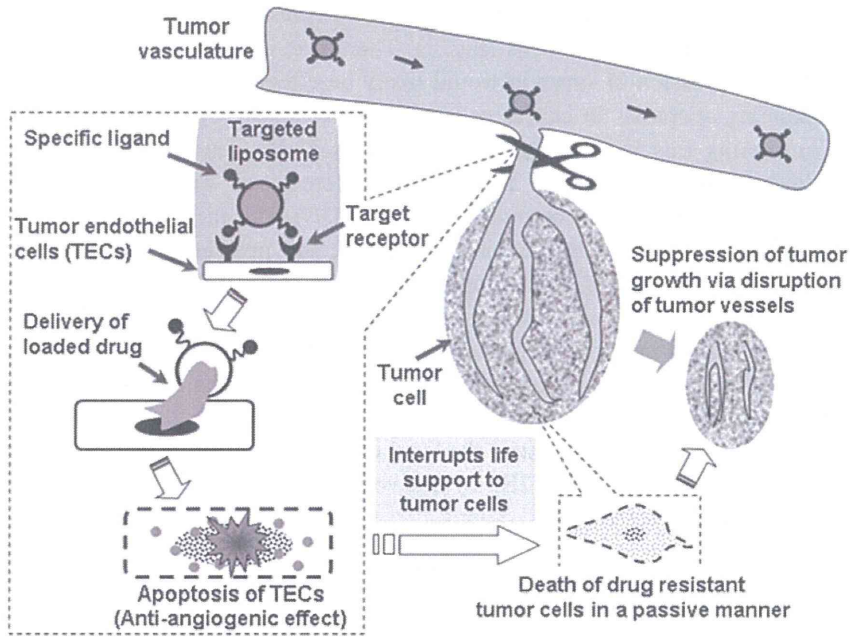

Fig. 3 Schematic illustration of the application of targeted anti-angiogenic therapy in the treatment of drug-resistant cancer. Ligand modified, drug-loaded nanoparticles deliver the drug and kill the TECs followed by the disruption of tumor blood vessels which supports the survival of tumor cells. The discontinuation of life supports leads the suppression of growth and progression of drug resistant tumor cells

desirable. TECs present in the tumor vasculatures provide life support to MDR tumor cells. Hence, targeting TECs would be an alternate and effective approach to the treatment of such types of notorious tumor cells (Figs. 2D, 3), where the drug is specifically delivered to the TECs via targeted nanoparticles, not to the MDR tumor cells.

Several specific markers, including integrin αvβ3, aminopeptidase N (CD13), vascular endothelial growth factor (VEGF) receptors (VEGF-R2, neuropilin-1), tumor endothelial markers (TEMs) etc. are expressed by TECs (Ruoslahti 2002) on their surfaces. Therefore, to target the TECs, ligand or antibody modified nanoparticles having ~100 dnm have been used to deliver a therapeutic moiety to TECs (Murphy et al. 2008; Pastorino et al. 2003). Antibody against the TEM8 marker exhibits an impaired growth of human tumor xenografts including melanoma, breast, colon, and lung cancer by the selective inhibition of pathological angiogenesis (Chaudhary et al. 2012). In another study, it was observed that cationic liposomes loaded with oxaliplatin provides ionic interactions with the surface molecules of TECs, resulting in a remarkable anti-angiogenic activity in mice bearing melanoma (B16BL6) tumors (Abu-Lila et al. 2009). Recently, an effective anti-angiogenic therapy has been developed in which K237 peptide-conjugated nanoparticles loaded with paclitaxel (K237-PTX-NP) were used to deliver the drug to the TECs for the treatment of P-gp overexpressing and paclitaxel resistant human colorectal adenocarcinoma (HCT-15) (Bai et al. 2013). These targeting approaches can be applied as an anti-angiogenic therapy (Fig. 3) for the treatment of MDR cancers.

In leaky tumor vasculatures, the length of the gaps in TECs varies, depending on the type of tumor. Therefore,

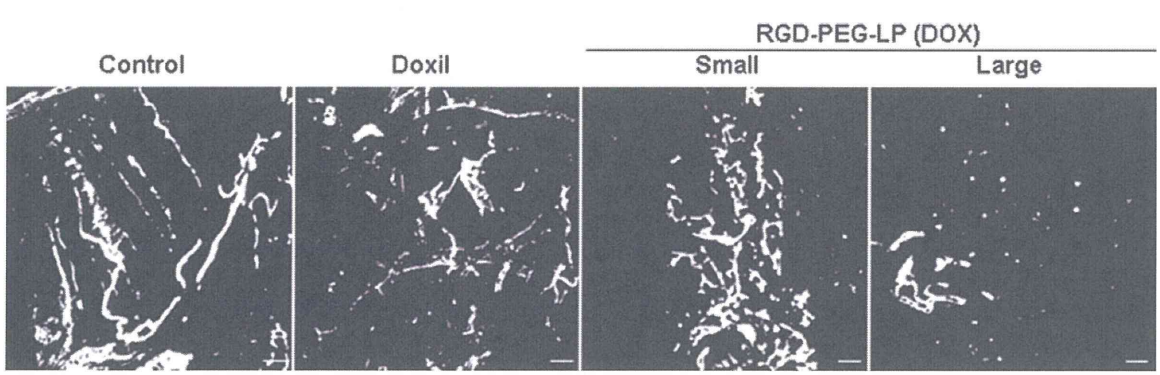

Fig. 4 Anti-angiogenic effect of DOX loaded PEG-LPs in DOX resistant human RCC tumor tissues. At a tumor volume of 150 mm^3 on the back of BALB/c male nude mice, 3 successive doses of 1.5 mg DOX/kg body weight were injected by tail vein. At 24 h post-injection, tumors were collected and observed under a microscope. Tumor blood vessels (*white*) were stained with FITC-isolectin B4; *scale bars* 50 μm. Large size RGD-PEG-LP (DOX) preferentially targets and delivers DOX to TECs followed by significant disruption of the tumor vasculatures as compared to others

the endothelial cell gap is an important issue to consider in designing nanoparticles for targeting TECs in a specific tumor type. For the treatment of DOX resistant renal cell carcinoma (RCC) via the targeting of TECs, we recently developed DOX loaded ligand modified size controlled PEG-LPs having ~300 dnm (Kibria et al. 2013; Takara et al. 2012). The large size particles (~300 dnm) showed a minimization of the EPR effect and preferentially targeted and delivered DOX to TECs, where the small size particles (~100 dnm) largely act directly on DOX-resistant tumor cells via the EPR effect. The DOX, delivered by large size particles, functions to kill the TECs, leading to the disruption of the tumor vasculature (Fig. 4), and discontinues life support to the tumor cells, ultimately causing the death (apoptosis) or inhibition of the growth of the RCC tumor cells in a blood supply-dependent manner (Fig. 3). Therefore, the targeted anti-angiogenic therapy using drug-loaded nanoparticles also has the promise of reversing the utilization of chemotherapeutic drugs for the treatment of chemotherapy resistant cancers.

Future perspectives

Due to self defense mechanisms, cancer cells show resistance to chemotherapeutic drugs for which the drug molecules eventually become ineffective, finally resulting in the failure of cancer treatment and thereby patient mortality. For reversing tumor cell resistance, it is immensely important to identify the key factors responsible for MDR in a specific tumor type. Based on a successful identification, it would be easier to design and apply DDS techniques to control the functions of the responsible factors, followed by the delivery of the chemotherapeutic drugs to which the cancer cells are resistant. Such a rationale design and application of DDS would permit cancer MDR to be overcome by making the cells chemosensitive as well as by reverting back the activity of drug molecules in MDR tumors.

Acknowledgments This study was supported in parts by grants from the Special Education and Research Expenses of the Ministry of Education, Culture, Sports, Science and Technology of Japan (MEXT); Nagai Foundation, Tokyo; as well as by a Grant-in-Aid for Research on Medical Device Development from the Ministry of Health, Labour and Welfare of Japan (MHLW).

References

Abu-Lila, A., T. Suzuki, Y. Doi, T. Ishida, and H. Kiwada. 2009. Oxaliplatin targeting to angiogenic vessels by PEGylated cationic liposomes suppresses the angiogenesis in a dorsal air sac mouse model. *Journal of Controlled Release* 134: 18–25.

Bai, F., C. Wang, Q. Lu, M. Zhao, F.Q. Ban, D.H. Yu, Y.Y. Guan, X. Luan, Y.R. Liu, H.Z. Chen, and C. Fang. 2013. Nanoparticle-mediated drug delivery to tumor neovasculature to combat P-gp expressing multidrug resistant cancer. *Biomaterials* 34: 6163–6174.

Bamias, A., and M.A. Dimopoulos. 2003. Angiogenesis in human cancer: Implications in cancer therapy. *European Journal of Internal Medicine* 14: 459–469.

Beck, A., M.C. Etienne, S. Cheradame, J.L. Fischel, P. Formento, N. Renee, and G. Milano. 1994. A role for dihydropyrimidine dehydrogenase and thymidylate synthase in tumour sensitivity to fluorouracil. *European Journal of Cancer* 30: 1517–1522.

Beck, W.T., M.K. Danks, J.S. Wolverton, R. Kim, and M. Chen. 1993. Drug resistance associated with altered DNA topoisomerase II. *Advances in Enzyme Regulation* 33: 113–127.

Borst, P., R. Evers, M. Kool, and J. Wijnholds. 2000. A family of drug transporters: The multidrug resistance-associated proteins. *Journal of the National Cancer Institute* 92: 1295–1302.

Boyle, P., and B. Levin. 2008. *World Cancer Report 2008*. Lyon: International Agency for Research on Cancer (IARC), 14–15.

Chabner, B.A., and T.G. Roberts. 2005. Timeline: Chemotherapy and the war on cancer. *Nature Reviews Cancer* 5: 65–72.

Chaudhary, A., M.B. Hilton, S. Seaman, D.C. Haines, S. Stevenson, P.K. Lemotte, W.R. Tschantz, X.M. Zhang, S. Saha, T. Fleming, and B. St Croix. 2012. TEM8/ANTXR1 blockade inhibits pathological angiogenesis and potentiates tumoricidal responses against multiple cancer types. *Cancer Cell* 21: 212–226.

Cherian, M.G., A. Jayasurya, and B.H. Bay. 2003. Metallothioneins in human tumors and potential roles in carcinogenesis. *Mutation Research* 533: 201–209.

Chin, J.L., D. Banerjee, S.A. Kadhim, T.E. Kontozoglou, P.J. Chauvin, and M.G. Cherian. 1993. Metallothionein in testicular germ cell tumors and drug resistance. Clinical correlation. *Cancer* 72: 3029–3035.

Choi, C.H. 2005. ABC transporters as multidrug resistance mechanisms and the development of chemosensitizers for their reversal. *Cancer Cell International* 5: 30.

Choi, H.S., W. Liu, F. Liu, K. Nasr, P. Misra, M.G. Bawendi, and J.V. Frangioni. 2010. Design considerations for tumour-targeted nanoparticles. *Nature Nanotechnology* 5: 42–47.

Clapper, M.L., S.J. Hoffman, and K.D. Tew. 1990. Sensitization of human colon tumor xenografts to L-phenylalanine mustard using ethacrynic acid. *Journal of Cellular Pharmacology* 1: 71–78.

Dalton, W.S. 1997. Mechanisms of drug resistance in hematologic malignancies. *Seminars in Hematology* 34: 3–8.

Danenberg, P.V. 1977. Thymidylate synthetase: A target enzyme in cancer chemotherapy. *Biochimica et Biophysica Acta* 473: 73–92.

Davis, M.E., Z.G. Chen, and D.M. Shin. 2008. Nanoparticle therapeutics: An emerging treatment modality for cancer. *Nature Reviews Drug Discovery* 7: 771–782.

Diestra, J.E., G.L. Scheffer, I. Català, M. Maliepaard, J.H. Schellens, R.J. Scheper, J.R. Germà-Lluch, and M.A. Izquierdo. 2002. Frequent expression of the multi-drug resistance associated protein BCRP/MXR/ABCP/ABCG2 in human tumours detected by the BXP-21 monoclonal antibody in paraffin-embedded material. *Journal of Pathology* 198: 213–219.

Dietel, M., H. Arps, H. Lage, and A. Niendorf. 1990. Membrane vesicle formation due to acquired mitoxantrone resistance in human gastric carcinoma cell line EPG85–257. *Cancer Research* 50: 6100–6161.

Di Paolo, D., C. Brignole, F. Pastorino, R. Carosio, A. Zorzoli, M. Rossi, M. Loi, G. Pagnan, L. Emionite, M. Cilli, S. Bruno, R. Chiarle, T.M. Allen, M. Ponzoni, and P. Perri. 2011. Neuroblastoma-targeted nanoparticles entrapping siRNA specifically knockdown ALK. *Molecular Therapy* 19: 1131–1140.

Doyle, L.A., W. Yang, L.V. Abruzzo, T. Krogmann, Y. Gao, A.K. Rishi, and D.D. Ross. 1998. A multidrug resistance transporter from human MCF-7 breast cancer cells. *Proceedings of the*

mediated drug delivery to tumor vasculature suppresses metastasis. *Proceedings of the National Academy of Sciences of the United States of America* 105: 9343–9348.

Nakamura, K., A.S. Abu Lila, M. Matsunaga, Y. Doi, T. Ishida, and H. Kiwada. 2011. A double-modulation strategy in cancer treatment with a chemotherapeutic agent and siRNA. *Molecular Therapy* 19: 2040–2047.

Pastorino, F., C. Brignole, D. Marimpietri, M. Cilli, C. Gambini, D. Ribatti, R. Longhi, T.M. Allen, A. Corti, and M. Ponzoni. 2003. Vascular damage and anti-angiogenic effects of tumor vessel-targeted liposomal chemotherapy. *Cancer Research* 63: 7400–7409.

Patil, Y., and J. Panyam. 2009. Polymeric nanoparticles for siRNA delivery and gene silencing. *International Journal of Pharmaceutics* 367: 195–203.

Patil, Y.B., S.K. Swaminathan, T. Sadhukha, L. Ma, and J. Panyam. 2010. The use of nanoparticle-mediated targeted gene silencing and drug delivery to overcome tumor drug resistance. *Biomaterials* 31: 358–365.

Patil, Y., T. Sadhukha, L. Ma, and J. Panyam. 2009. Nanoparticle-mediated simultaneous and targeted delivery of paclitaxel and tariquidar overcomes tumor drug resistance. *Journal of Controlled Release* 136: 21–29.

Peer, D., J.M. Karp, S. Hong, O.C. Farokhzad, R. Margalit, and R. Langer. 2007. Nanocarriers as an emerging platform for cancer therapy. *Nature Nanotechnology* 2: 751–760.

Persidis, A. 1999. Cancer multidrug resistance. *Nature Biotechnology* 17: 94–95.

Raaijmakers, H.G., M.A. Izquierdo, H.M. Lokhorst, C. de Leeuw, J.A. Belien, A.C. Bloem, A.W. Dekker, R.J. Scheper, and P. Sonneveld. 1998. Lung-resistance-related protein expression is a negative predictive factor for response to conventional low but not to intensified dose alkylating chemotherapy in multiple myeloma. *Blood* 91: 1029–1036.

Rajagopal, A., and S.M. Simon. 2003. Subcellular localization and activity of multidrug resistance proteins. *Molecular Biology of the Cell* 14: 3389–3399.

Rejman, J., V. Oberle, I.S. Zuhorn, and D. Hoekstra. 2004. Size-dependent internalization of particles via the pathways of clathrin- and caveolae-mediated endocytosis. *Biochemical Journal* 377: 159–169.

Rezzani, R. 2004. Cyclosporine A and adverse effects on organs: Histochemical studies. *Progress in Histochemistry and Cytochemistry* 39: 85–128.

Ruoslahti, E. 2002. Specialization of tumour vasculature. *Nature Reviews Cancer* 2: 83–90.

Saad, M., O.B. Garbuzenko, and T. Minko. 2008. Co-delivery of siRNA and an anticancer drug for treatment of multidrug-resistant cancer. *Nanomedicine (London)* 3: 761–776.

Salonga, D., K.D. Danenberg, M. Johnson, R. Metzger, S. Groshen, D.D. Tsao-Wei, H.J. Lenz, C.G. Leichman, L. Leichman, R.B. Diasio, and P.V. Danenberg. 2000. Colorectal tumors responding to 5-fluorouracil have low gene expression levels of dihydropyrimidine dehydrogenase, thymidylate synthase, and thymidine phosphorylase. *Clinical Cancer Research* 6: 1322–1327.

Scheffer, G.L., A.B. Schroeijers, M.A. Izquierdo, E.A. Wiemer, and R.J. Scheper. 2000. Lung resistance-related protein/major vault protein and vaults in multidrug-resistant cancer. *Current Opinion in Oncology* 12: 550–556.

Sharma, A., E. Mayhew, and R.M. Straubinger. 1993. Antitumor effect of taxol-containing liposomes in a taxol-resistant murine tumor model. *Cancer Research* 53: 5877–5881.

Shen, F., S. Chu, A.K. Bence, B. Bailey, X. Xue, P.A. Erickson, M.H. Montrose, W.T. Beck, and L.C. Erickson. 2008. Quantitation of doxorubicin uptake, efflux, and modulation of multidrug resistance (MDR) in MDR human cancer cells. *Journal of Pharmacology and Experimental Therapeutics* 324: 95–102.

Shimoda, R., W.E. Achanzar, W. Qu, T. Nagamine, H. Takagi, M. Mori, and M.P. Waalkes. 2003. Metallothionein is a potential negative regulator of apoptosis. *Toxicological Sciences* 73: 294–300.

Shintani, Y., M. Ohta, H. Hirabayashi, H. Tanaka, K. Iuchi, K. Nakagawa, H. Maeda, T. Kido, S. Miyoshi, and H. Matsuda. 2003. New prognostic indicator for non-small-cell lung cancer, quantitation of thymidylate synthase by real-time reverse transcription polymerase chain reaction. *International Journal of Cancer* 104: 790–795.

Siwak, D.R., A.M. Tari, and G. Lopez-Berestein. 2002. The potential of drug-carrying immunoliposomes as anticancer agents. *Clinical Cancer Research* 8: 955–956.

Smith, K., S. Houlbrook, M. Greenall, J. Carmichael, and A.L. Harris. 1993. Topoisomerase IIα coamplification with erbB2 in human primary breast cancer and breast cancer cell lines -relationship to m-AMSA and mitoxantrone sensitivity. *Oncogene* 8: 933–938.

Soma, C.E., C. Dubernet, D. Bentolila, S. Benita, and P. Couvreur. 2000. Reversion of multidrug resistance by co-encapsulation of doxorubicin and cyclosporin A in polyalkylcyanoacrylate nanoparticles. *Biomaterials* 21: 1–7.

Sugahara, S., M. Kajiki, H. Kuriyama, and T.R. Kobayashi. 2007. Complete regression of xenografted human carcinomas by a paclitaxel-carboxymethyl dextran conjugate (AZ10992). *Journal of Controlled Release* 117: 40–50.

Takara, K., H. Hatakeyama, G. Kibria, N. Ohga, K. Hida, and H. Harashima. 2012. Size-controlled, dual-ligand modified liposomes that target the tumor vasculature show promise for use in drug-resistant cancer therapy. *Journal of Controlled Release* 162: 225–232.

Tewey, K.M., T.C. Rowe, L. Yang, B.D. Halligan, and L.F. Liu. 1984. Adriamycin-induced DNA damage mediated by mammalian DNA topoisomerase II. *Science* 226: 466–468.

Toyoda, Y., Y. Hagiya, T. Adachi, K. Hoshijima, M.T. Kuo, and T. Ishikawa. 2008. MRP class of human ATP binding cassette (ABC) transporters: Historical background and new research directions. *Xenobiotica* 38: 833–862.

Walther, W., U. Stein, and H. Lage. 2010. Jet-injection of short hairpin RNA-encoding vectors into tumor cells. *Methods in Molecular Biology* 629: 123–139.

Wang, R.B., C.L. Kuo, L.L. Lien, and E.J. Lien. 2003. Structure-activity relationship: Analyses of p-glycoprotein substrates and inhibitors. *Journal of Clinical Pharmacy and Therapeutic* 28: 203–228.

Wang, Y., S. Gao, W.H. Ye, H.S. Yoon, and Y.Y. Yang. 2006. Co-delivery of drugs and DNA from cationic core-shell nanoparticles self-assembled from a biodegradable copolymer. *Nature Materials* 5: 791–796.

Wang, Z., Y. Li, A. Ahmad, A.S. Azmi, D. Kong, S. Banerjee, and F.H. Sarkar. 2010. Targeting mirnas involved in cancer stem cell and EMT regulation: An emerging concept in overcoming drug resistance. *Drug Resistance Updates* 13: 109–118.

Wright, J.A., H.S. Smith, F.M. Watt, M.C. Hancock, D.L. Hudson, and G.R. Stark. 1990. DNA amplification is rare in normal human cells. *Proceedings of the National Academy of Sciences of the United States of America* 87: 1791–1795.

Wu, J., Y. Lu, A. Lee, X. Pan, X. Yang, X. Zhao, and R.J. Lee. 2007. Reversal of multidrug resistance by transferrin-conjugated liposomes co-encapsulating doxorubicin and verapamil. *Journal of Pharmacy and Pharmaceutical Sciences* 10: 350–357.

Yamachika, T., H. Nakanishi, K. Inada, T. Tsukamoto, T. Kato, M. Fukushima, M. Inoue, and M. Tatematsu. 1998. A new prognostic factor for colorectal carcinoma, thymidylate synthase, and its therapeutic significance. *Cancer* 82: 70–77.

Yuan, F., M. Leunig, S.K. Huang, D.A. Berk, D. Papahadjopoulos, and R.K. Jain. 1994. Microvascular permeability and interstitial

penetration of sterically stabilized (Stealth®) liposomes in a human tumor xenografts. *Cancer Research* 54: 3352–3356.

Zhang, B., M. Liu, H.K. Tang, H.B. Ma, C. Wang, X. Chen, and H.Z. Huang. 2012. The expression and significance of MRP1, LRP, TOPOIIβ, and BCL2 in tongue squamous cell carcinoma. *Journal of Oral Pathology and Medicine* 41: 141–148.

Zhang, L., F.X. Gu, J.M. Chan, A.Z. Wang, R.S. Langer, and O.C. Farokhzad. 2008. Nanoparticles in medicine: therapeutic applications and developments. *Clinical Pharmacology and Therapeutics* 83: 761–769.

Zhou, S.F. 2008. Structure, function and regulation of P-glycoprotein and its clinical relevance in drug disposition. *Xenobiotica* 38: 802–832.

Journal of Controlled Release 173 (2014) 110–118

Contents lists available at ScienceDirect

Journal of Controlled Release

journal homepage: www.elsevier.com/locate/jconrel

RNAi-mediated gene knockdown and anti-angiogenic therapy of RCCs using a cyclic RGD-modified liposomal-siRNA system

Yu Sakurai [a], Hiroto Hatakeyama [a], Yusuke Sato [a], Mamoru Hyodo [a], Hidetaka Akita [a], Noritaka Ohga [b], Kyoko Hida [b], Hideyoshi Harashima [a,*]

[a] Laboratory of Innovative Nanomedicine, Faculty of Pharmaceutical Sciences, Hokkaido University, Kita 12, Nishi 6, Kita-ku, Sapporo 060-0812, Japan
[b] Division of Vascular Biology, Graduate School of Dental Medicine, Hokkaido University, Kita 13 Nishi 7, Kita-ku, Sapporo 060-0812, Japan

ARTICLE INFO

Article history:
Received 21 May 2013
Accepted 3 October 2013
Available online 11 October 2013

Keywords:
siRNA
Liposome
Anti-angiogenic therapy
Cyclic RGD
Active targeting

ABSTRACT

Angiogenesis is one of crucial processes associated with tumor growth and development, and consequently a prime target for cancer therapy. Although tumor endothelial cells (TECs) play a key role in pathological angiogenesis, investigating phenotypical changes in neovessels when a gene expression in TEC is suppressed is a difficult task. Small interfering RNA (siRNA) represents a potential agent due to its ability to silence a gene of interest. We previously developed a system for *in vivo* siRNA delivery to cancer cells that involves a liposomal-delivery system, a MEND that contains a unique pH-sensitive cationic lipid, YSK05 (YSK-MEND). In the present study, we report on the development of a system that permits the delivery of siRNA to TECs by combining the YSK-MEND and a ligand that is specific to TECs. Cyclo(Arg-Gly-Asp-D-Phe-Lys) (cRGD) is a well-known ligand to $\alpha_V\beta_3$ integrin, which is selectively expressed at high levels in TECs. We incorporated cRGD into the YSK-MEND (RGD-MEND) to achieve an efficient gene silencing in TECs. Quantitative RT-PCR and the 5′ rapid amplification of cDNA ends PCR indicated that the intravenous injection of RGD-MEND at a dose of 4.0 mg/kg induced a significant RNAi-mediated gene reduction in TEC but not in endothelial cells of other organs. Finally, we evaluated the therapeutic potency of the RGD-MEND encapsulating siRNA against vascular endothelial growth factor receptor 2. A substantial delay in tumor growth was observed after three sequential RGD-MEND injections on alternate days. In conclusion, the RGD-MEND represents a new approach for the characterization of TECs and for us in anti-angiogenic therapy.

1. Introduction

Angiogenesis is a major cause in cancer progression and metastasis [1,2]. Folkman et al. first proposed the theory that, to be supplied with oxygen and other nutrients, tumors with sizes over 1–2 mm^3 inevitably required angiogenesis, and that, if tumor vasculature development could be inhibited, tumor tissue would shrink, as the result of a lack of oxygen and other nutrients [3]. Since this publication, anti-angiogenic therapy has evolved as an innovative treatment for various cancers. A mono-clonal antibody against vascular endothelial growth factor (VEGF), which is referred to as Avastin, is currently used in the treatment of various types of cancer [4,5].

Small interfering RNA (siRNA) was predicted to be a potentially useful drug for this purpose, due to the ability to inhibit the expression of any genes of interest in a sequence-specific manner [6]. However, its instability in the blood and the low permeability of the plasma membrane require drug delivery systems that target specific cells in order to achieve an effective therapy by siRNA [6,7]. We previously developed a liposomal siRNA system, a multi functional nano-device (MEND) [8,9]. In the past report, the use of a MEND composed of a pH-sensitive cationic lipid, YSK05 (YSK-MEND) caused a significant gene reduction in tumor tissue when intratumorally and intravenously injected into tumor-bearing mice [10,11]. A number of pH sensitive siRNA carriers, such as liposomes [12,13], polyplexes [14] and micelles [15], have been evaluated for use in tumor targeting. pH-sensitive carriers are generally thought to be more suitable for tumor targeting than conventional cationic carriers because of their highly specific fusiogenicity in acidic endosomes [16]. YSK05 consists of two linoleyl fatty acid chains and a tertiary amino group, which are responsible for pH-responsive fusiogenicity in endosomes. In this study, we incorporated a ligand that is specific to tumor endothelial cells (TECs) into YSK-MEND to achieve anti-angiogenic therapy using siRNA.

Cyclo (Arg-Gly-Asp-D-Phe-Lys) (cRGD) peptide is a well-validated ligand for $\alpha_V\beta_3$ integrin, which is highly and selectively expressed on the cell surface of TECs and some types of cancer cells themselves [17]. cRGD is a known antagonist of $\alpha_V\beta_3$ integrin, and the injection of free cRGD suppresses tumor progression in many cancers such as glioblastomas and lung cancer [18]. This is because $\alpha_V\beta_3$ integrin plays a key role in angiogenesis in tumor tissue [19]. Moreover, the cRGD peptide can be

* Corresponding author at: Kita-12, Nishi-6, Kita-ku, Sapporo 060-0812, Japan. Tel.: +81 11 706 3919; fax: +81 11 706 4879.
E-mail address: harasima@pharm.hokudai.ac.jp (H. Harashima).

0168-3659/$ – see front matter © 2013 Elsevier B.V. All rights reserved.
http://dx.doi.org/10.1016/j.jconrel.2013.10.003

used for a variety of purposes, including cancer imaging and therapy by conjugating cRGD with imaging probes, anti-cancer agents or drug carriers [20]. Concerning the *in vivo* delivery of nucleic acids using cRGD, several reports have appeared in which tumor growth was inhibited by the systemic injection of anti-tumor and/or anti-angiogenic oligonucleotides encapsulated in micelles [21] and lipoplexes [22–24]. However, in almost all of those reports it was not clear whether siRNA was delivered to cancer cells and TECs, and no direct evidence showing that a gene reduction in TECs was mediated by RNA interference. In this study, we verified gene silencing by siRNA in TECs using quantitative RT-PCR (qRT-PCR) and rapid amplification of the 5′ cDNA ends (5′ RACE-PCR), which was the only method available for confirming RNAi-induced silencing [7].

We chose renal cell carcinomas (RCCs) as a therapeutic model cancer by inhibiting angiogenesis, since it is well known that RCCs effectively respond to anti-angiogenic therapy [25]. Since RCCs are known to respond poorly to conventional anti-cancer drugs, interleukin-2 and interferon-α injections are currently the standard treatment for patients with progressive RCCs [26]. In recent years, however, novel agents targeting angiogenesis pathways have been developed as the result in advances in our understanding of tumor biology. Actually, Afinitor and Toricel (mTOR inhibitors) and Sutent (a multi kinase inhibitor) are currently being applied for metastatic RCCs in addition to Avastin.

Although anti-angiogenic treatment has had significant therapeutic effects for cancer progress and metastasis, it has been reported that some patients are refractory or acquire resistance to VEGF inhibition [27]. Several mechanisms are thought to be involved in the resistance anti-angiogenic treatment by VEGF blockade. Compensation by other pro-angiogenic mechanisms, such as basic fibloblast growth factors (bFGF), platelet-derived growth factor (PDGF) and angiopoietins, appears to be a dominant factor in the development of acquired resistance to VEGF inhibition. Moreover, recent reports suggest that the recruitment of other cells, such as pericytes and bone marrow-derived myeloid cells, to tumor vessels is implicated in the resistance to anti-angiogenic therapy [28,29]. A methodology that will permit the complete control any gene that is expressed in TECs is needed for further elucidating the mechanism of anti-angiogenic therapy resistance, and hence developing a better therapy that targets tumor angiogenesis. In the study, we report that the RGD-MEND represents an efficient siRNA delivery system for cancer treatment through anti-angiogenic therapy.

2. Materials and methods

2.1. Materials

1,2-Distearoyl-sn-glycerophosphocholine (DSPC), 1-palmitoyl-2-oleoyl-sn-glycerophosphoethanolamine (POPE), 1,2-dimyristoyl-sn-glycerol, methoxypolyethylene glycol$_{2000}$ (PEG-DMG), 1,2-distearoyl-sn-glycerol, methoxypolyethylene glycol$_{2000}$ (PEG-DSG) and N-hydroxysuccinimide-polyethylene glycol$_{2000}$-1,2-disteaoyl-sn-glycerophosphoethanolamine (NHS-PEG-DSPE) were purchased NOF (Tokyo, Japan). Cholesterol (chol), RPMI-1640 medium and DMEM were obtained from SIGMA Aldrich (St. Louis, MO). Egg phosphatidyl choline (EPC) and 1,2-distearoyl-sn-grycelo, methoxy polyethylene glycol (PEG-DSPE) were purchased from Avanti Polar Lipids (Alabaster, AL). siRNAs were obtained from Hokkaido System Science Co., Ltd. (Sapporo, Japan). [^{3}H]-choresteryl hexadecyl ether (CHE) was purchased from PerkinElmer Life Science (Tokyo, Japan). DiI and DiD were purchased from Invitrogen (Carlsbad, CA).

2.2. Synthesis of cRGD conjugates

We synthesized cRGD-conjugated PEG (RGD-PEG) as previously reported [30]. In brief, cRGD peptide was incubated with NHS-PEG-DSPE in 20 mM phosphate buffered saline (pH 7.4, PBS) at 37 °C for 12 h. The mixture was then subject to dialysis using Spectra Por 6 (MWCO 1000 Da, Spectrum) to remove un-conjugated RGD. The molecular weight of the conjugate was determined by MALDI TOF-MS.

2.3. MEND preparation

YSK-MENDs were prepared as previously reported [10,11]. Briefly, 1500 nmol of YSK05, 750 nmol of POPE, 750 nmol chol and 150 nmol PEG-DMG were dissolved in 400 μL of 90% (v/v) aqueous tertiary butanol (t-BuOH). When the fluorescence was incorporated into the YSK-MENDs, 0.5 mol% (of the total lipid) DiD was added to the tubes and the organic solvent was removed by evaporation before the lipid solution was mixed. Two hundred microliters of siRNA solution (concentration 0.8 mg/mL in 2 mM filter-sterilized citrate buffer (pH4.5)) was gradually added to the shaking lipid solution, and homogenous particles of liposomal siRNA were spontaneously formed by drastically diluting the siRNA–lipid mixture to 2 mL with 20 mM citrate buffer. The t-BuOH was then removed by ultrafiltration. For RGD-modification, a RGD–PEG solution was incubated with a YSK-MEND solution at 60 °C for 30 min at various molar ratios (RGD-PEG/total lipid of YSK-MEND). The YSK-MENDs were characterized by a Zetasizer Nano ZS ZEN3600 instrument (Malvern Instruments, Worchestershire, UK). The encapsulation efficiency and recovery ratio were calculated using RiboGreen (Invitrogen) as previously described [10]. siRNA encapsulation efficiency rate of all MENDs used in this study was over 90%. The sequences of the used siRNAs are shown in Supplemental Table S1.

2.4. Cell culture

OS-RC-2 cells and HEK293T cells were cultured in RPMI-1640 and DMEM, respectively. These media were supplemented with 10% fetal bovine serum, penicillin (100 U/mL) and streptomycin (100 μg/mL). TECs, which were previously isolated by Ohga et al. [31], and HUVEC were cultured in EBM-2 medium supplemented with 2% FBS (v/v) and bullet kits (Lonza, Walkersville, MD). All cells were maintained at 37 °C in a 5% CO_2 humidified atmosphere.

2.5. Evaluation of antigen expression

For evaluating the expression of $\alpha_V\beta_3$ integrin, 1.0×10^6 trypsinized cells were suspended in 1 mL of FACS buffer (0.5% bovine serum albumin and 0.1% sodium azide in 20 mM PBS), and the suspension was centrifuged at 4 °C for 4 min at 500 × g. The cells were incubated in 100-fold diluted anti human $\alpha_V\beta_3$ integrin rat IgG (R&D systems, Minneapolis, MN) for 30 min on ice. The antibody solution was then removed by centrifugation and the cells were washed twice with 500 μL of FACS buffer. Two hundred-fold diluted Alexa633-labeled anti rat IgG goat F(ab′) (Invitrogen) was added to the cells. The cells were washed twice with 500 μL of FACS buffer, and re-suspended in 1 mL of FACS buffer. The cell suspension was analyzed by FACSCalibur (Becton Dickinson, Franklin Lakes, NJ).

2.6. Animal study

Male, 4-week-old ICR mice and BALB/cAJcl-*nu/nu* were purchased from Japan SLC (Shizuoka, Japan) and CLEA (Tokyo, Japan), respectively. For preparing OS-RC-2-bearing mice, 1.0×10^6 OS-RC-2 cells in 75 μL of sterilized PBS were inoculated into anesthetized BALB/cAJcl-*nu/nu* mice on the right flank. The experimental protocols were reviewed and approved by the Hokkaido University Animal Care Committee in accordance with the Guide for the Care and Use of Laboratory Animals.

2.7. Confocal laser scanning microscopy (CLSM) to determine the localization in tumor tissue of the MEND

OS-RC-2-bearing mice were intravenously administered with 3.0 mg/kg of DiD labeled-YSK-MEND. FITC-labeled Isolectin B4 (Vector Laboratories, Burlingame, CA) were injected via the tail vein 10 min before collecting. Tumor tissue was excised 24 h after injection of the YSK-MENDs, and then fixed with 4% paraformaldehyde (PFA). Fixed tumor tissue was washed with 10%, 30% and 50% sucrose over night. Tumor tissue was embedded in OCT compound, and 16 μm thick slices were prepared on the slideglass SUPERFROST S9441 (MATUSNAMI) with CM-3050S (Leica, Wetzlar, Germany). Tumor slices were washed with PBS twice, and covered with a cover glass. The tumor slices were observed with an FV10i-LIV microscope.

2.8. Flowcytometry (FCM) analysis for the internalization of MEND into cells

To investigate the localization of the YSK-MENDs in tumor tissue after systemic injection, OS-RC-2 bearing mice were systemically injected with DiD labeled-YSK-MENDs at a dose of 3 mg/kg. Tumor tissue was collected 6 h after injection, and then shredded. The shredded tumor tissue was then incubated in 2 mL of Hanks' Balanced Salt Solution (HBSS, SIGMA Aldrich) containing 20 mg of type I collagenase (Gibco, Rockville, MD), 200 μg of DNase I (Gibco), 1 mL of inactivated FBS and 2.0 mmol of $CaCl_2$ for 30 min at 37 °C. The resulting cell suspension was filtered through a 100 μm Cell Strainer (BD Falcon), and then centrifuged at 4 °C for 3 min at 500 rpm after the addition of 10 mL of HBSS and the supernatant was removed. This "washing procedure" was repeated 2 times. To remove red blood cells, the centrifuged cells were incubated in Red Blood Cell Lysing Buffer (SIGMA Aldrich) for a several minutes at room temperature and the washing procedure was repeated once. Next, 1.0×10^6 cells were incubated with an anti mouse PE-labeled CD31 antibody (Biolegend, San Diego, CA) or PE-labeled Rat IgG2a, κ isotype control (Biolegend) for 30 min on ice. Cells were washed, and then analyzed with FACSCalibur 10 min after 7-AAD (IMGENEX, San Diego, CA) addition. The 7-AAD-positive population was assumed to be dead cells and were gated out.

2.9. Evaluation for gene silencing by qRT-PCR

Cells plated onto 6-well plate were lysed by treatment with 350 μL of TRIzol (Invitrogen). For the *in vivo* experiment, approximately 50 mg of collected tissue was homogenized by means of a PreCellys (Bertin Technologies, Montigny-Le-Bretonneux, France) in 500 μL of TRIzol, and then centrifuged at 12,000 ×*g* at 4 °C for 15 min. Supernatant was used as an RNA extraction sample. RNA extraction and purification was then performed according to the manufacturers' protocol. One microgram of total RNA was subjected to reverse transcription reaction using a High Capacity RNA-to-cDNA kit (Applied Biosystems, Foster City, CA).

Fifty-fold diluted cDNA was subject to qPCR with Fast SYBR Green Master Mix (Applied Biosystems) using LightCycler-480 (Roche Diagnostics, Germany). The reaction conditions were according to the manufacturer's protocol. The sequences of all primer sets in the experiment are shown in Supplemental Table S1.

2.10. Confirmation of RNAi-mediated gene silencing by 5′ RACE-PCR

5′ RACE-PCR for the detection of *Cd31* mRNA cleaved by si-*Cd31* was carried out as previously reported [11]. Briefly, GeneRacer Adaptor was ligated into cleaved *Cd31* mRNA, and then reverse transcribed with *Cd31* Gene Specific Primer by SuperScript III (Invitrogen). Next, cDNA was amplified by 2 times PCR (i.e. nested PCR) with 2 different sets of PCR primers (Ad5 outer and *Cd31* outer primers for the 1st PCR, and Ad5 inner and *Cd31* inner primers for the 2nd PCR). All oligonucleotides used in the procedure are shown in Supplemental Table S1.

2.11. Somatic and hepatic toxicity

Liver toxicity was evaluated 24 h after injection of the MEND at a dose of 3.0 mg/kg. Serum asparate aminotransferase (AST) and alanine aminotransferase (ALT) were measured using a transaminase CII test kit (Wako Pure Chemicals, Osaka, Japan) in accordance with manufacturer's instructions.

2.12. Statistical analysis

Comparisons between multiple treatments were made using one-way ANOVA, followed by the Bonferroni test. Pair-wise comparisons between treatments were made using a Student's *t*-test. A p-value of <0.05 was considered significant.

3. Results

3.1. Preparation and characterization of YSK-MEND modified with RGD-PEG (RGD-MEND)

The expression of integrin $\alpha_V\beta_3$ in two cell lines was determined by FCM (Fig. 1).

We next evaluated the optimal modification ratio of RGD-PEG into the YSK-MEND at 0–10 mol% against the total lipid. The lipid composition of the YSK-MEND was YSK05/POPE/chol/PEG-DMG (50/25/25/3, molar ratio), which showed the most efficient silencing effect in the *in vitro* cultured cell line [10]. The PEG-DSPE (without cRGD) modified YSK-MEND (PEG-MEND) was regarded as a negative control in the *in vitro* study. The characteristics of these RGD-MENDs are shown in Table 1. In HUVEC, a 5.0 mol% modification facilitated the cellular internalization of the YSK-MEND to the greatest extent (Fig. 2). However, a further increase was not observed when the modification ratio was 10 mol% against the total lipid. On the other hand, no change in the cellular uptake of nanoparticles was observed in the case of HEK293T cells. We also carried out this cellular uptake experiment with RGD-modified liposomes (Fig. S1), and similar results were observed in FCM and CLSM studies. Taken together, we conclude that the RGD-incorporation ratio was 5.0 mol%. In addition, RGD-modification had no effect on the pH-sensitivity of the YSK-MEND (Fig. S2). Next, we evaluated the knockdown effect of RGD-MEND. Anti polo-like kinase 1 siRNA (si-*PLK1*) formulated into both RGD-MEND and PEG-MEND was added to HUVEC and HEK293T at a concentration of 11–100 nM. Anti-luciferase siRNA (si-*luc*) was used as a negative control siRNA. The

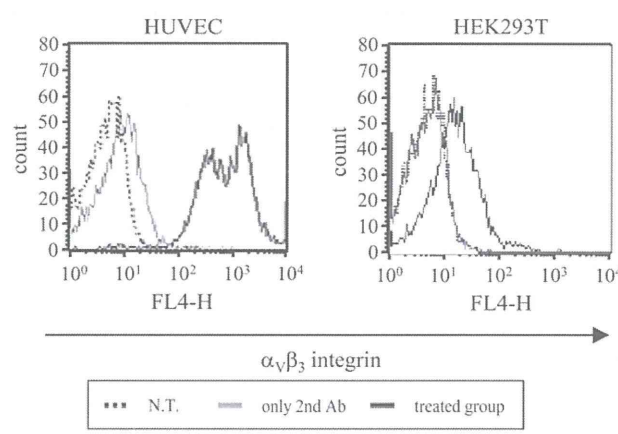

Fig. 1. $\alpha_V\beta_3$ integrin expression in HUVEC and HEK293T cells. HUVEC (left panel) and HEK293T (right panel) were treated with anti-$\alpha_V\beta_3$ integrin antibody and s fluorescence labeled-2nd antibody, and then analyzed by FCM. In the histograms, the black dotted line, the black solid line and the gray solid line denote untreated cells, cells treated with both the 1st and 2nd antibody and cells treated with only the 2nd antibody, respectively. N.T.: non treatment.

Table 1
Characteristics of the RGD-MENDs used in the *in vitro* cellular uptake experiments.

	RGD-modified MEND				
Lipid composition	YSK05/POPE/chol/PEG-DMG 50/25/25/3				
RGD-PEG (mol%)	0	1.0	2.5	5.0	10
Diameter (nm)	106 ± 6	107 ± 8	106 ± 10	101 ± 3	110 ± 12
PdI	0.10 ± 0.02	0.15 ± 0.01	0.16 ± 0.04	0.13 ± 0.02	0.22 ± 0.05
ζ-potential (mV)	−5 ± 3	−6 ± 5	−9 ± 10	−11 ± 4	−13 ± 8

Data represents mean ± SD.

RGD-MEND reduced target gene expression in a dose-dependent manner, while the PEG-MEND caused no detectable changes in target gene expression in HUVEC (Fig. 3A). In the case of HEK293T, however, neither the PEG-MEND nor the RGD-MEND induced gene silencing (Fig. 3B). On the other hand, si-*PLK1* transfection with RNAiMAX significantly inhibited *PLK1* expression in HEK293T cells (Fig. S3). This result clearly shows that HEK293T was not refractory to si-*PLK1*.

3.2. Localization of RGD-MEND after systemically injection

We next investigated the tumor accumulation of RGD-MEND intravenously injected into mice. Tumor distribution was observed by CLSM and FCM in order to detect the specific delivery siRNA to TECs, not tumor whole tissue. To evaluate the targeting potency of the RGD-MEND, we compared with active targeting RGD-MEND with a "cancer cell targeting" YSK-MEND (a conventional YSK-MEND), which was originally developed for silencing cancer cell genes [11]. Generally speaking, liposomes with a prolonged circulation time after systemic injection can passively accumulate and diffuse in tumor tissue through the enhanced permeability and retention (EPR) effect [32]. The EPR effect is caused by increasing vessel permeability and decreasing lymphatic drainage in tumor tissue due to the development of an aberrant tumor vasculature. The conventional YSK-MEND could circulate in blood stream as previously shown [11], and consequently accumulated and spread in tumor tissue. Therefore, the non-active targeting conventional YSK-MEND achieved "cancer cell targeting" via the EPR effect, which resulted in a significant gene silencing in cancer cells. In addition, we previously reported that non-ligand PEG-MEND (YSK05/POPE/chol/PEG-DMG 50/25/25/3) was not able to deliver siRNA in target organs, and concluded that the PEG-MEND could not be used as a negative control in the *in vivo* study. Taken together, in the *in vivo* section, the conventional YSK-MEND was regarded as a control non-TEC targeting carrier. The characteristics and lipid composition of the MENDs used in the *in vivo* experiments are shown in Table 2. Actually we were not able to observe the effective knockdown in TECs after the injection of the conventional YSK-MEND (Fig. S4). In TECs, the DiD signal was detected only in the group treated with the RGD-MEND (Fig. 4A). In addition, the RGD-MEMD was co-localized with TECs (Figs. 4B, S5). However, the intravenously injected conventional YSK-MEND was not observed in TECs but was diffused over the entire tumor tissue. To demonstrate the effect of cRGD, we also investigated the targeting ability and the knockdown efficiency of the PEG-MEND (YSK-MEND modified with PEG-DSPE instead of RGD-PEG). The systemically injected PEG-MEND neither accumulated in TECs (Fig. S6A) nor inhibited TECs-specific gene expression (Fig. S6B).

Regarding the distribution in other organs, a high accumulation of systemically administered RGD-MEND was detected in the liver, spleen and lungs (Fig. S7).

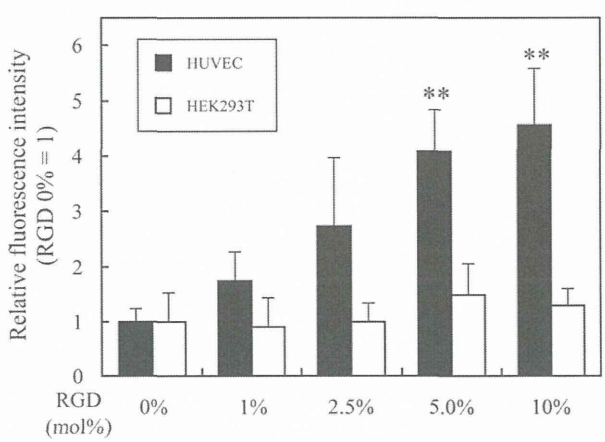

Fig. 2. Cellular uptake of RGD-MENDs containing various amounts of RGD-PEG. Cellular uptake was determined by FCM at 3 h after adding the fluorescence-labeled MENDs to the cells. In the graph, the fluorescence intensity was normalized to RGD 0% in each cell line. White columns and black columns indicate the cellular uptake of HUVEC and that of HEK293T, respectively. **: $p < 0.01$ (ANOVA followed by Bonferroni correction vs. RGD 0% in HUVEC. $n = 3$).

3.3. Selective gene silencing of systemic administered RGD-MEND

We then evaluated the *in vivo* knockdown and therapeutic effect of the RGD-MEND. To specifically determine the extent of gene knockdown in TECs, *Cd31*, which is selectively expressed in both TECs and normal endothelial cells (ECs), was used. OS-RC-2-bearing mice were treated with anti *Cd31* siRNA (si-*Cd31*) encapsulated in the RGD-MEND at a dose ranging from 0.5 to 4.0 mg/kg. As a result, the RGD-MEND caused a reduction in *Cd31* expression in a dose-dependent manner while the si-*luc* encapsulated in RGD-MEND did not (Fig. 5A). In contrast, RGD-MEND did not downregulate the gene in cancer cells (Fig. S8). Furthermore, we confirmed that this inhibition was caused by RNAi with 5′ RACE-PCR (Fig. 5B). As a result of a 5′ RACE-PCR experiment, approximately 250 bp of PCR products were obtained at a dose of 4.0 mg/kg. Thus, the reduction in *Cd31* expression can be attributed to an RNAi-mediated mechanism (Fig. 5C). To evaluate the possibility that RGD-MEND injection causes side effects, we investigated the silencing effect of other organs' ECs. However, no inhibitory effect on the siRNA-target gene was observed in these tissues (Fig. S9).

3.4. Therapeutic effect of si-Vegfr2 encapsulated in the RGD-MEND

Finally, we examined the therapeutic effect of the RGD-MEND. *VEGFR2* is one of the dominant factors in angiogenesis, and the inhibition of VEGFR2 by an antibody induced anti-tumor effect via thorough inhibition of angiogenesis including RCCs [33,34]. Therefore, we chose *VEGFR2* as a therapeutic gene in this tumor model. The sequence of the anti *Vegfr2* siRNA was determined by comparing the gene silencing effect in cultured TECs (Fig. S10A). Then, OS-RC-2-bearing mice were daily injected twice with the most effective anti *Vegfr2* siRNA (si-*Vegfr2*) encapsulated in the RGD-MEND at a concentration of 3.0 mg/kg. As a result, a significant *Vegfr2* knockdown was observed *in vivo* (Fig. S10B). Additionally, si-*Vegfr2* had no effect on the viability of OS-RC-2 itself (Fig. S11). Then, when we monitored tumor growth after 3 injections of si-*Vegfr2* encapsulated in the RGD-MEND, a significant delay in tumor growth was observed (Fig. 6A). The si-*Vegfr2* treatment significantly lowered the amount